TECHNICAL REPORT R-12

EFFECT OF THE PROXIMITY OF THE WING FIRST-BENDING FREQUENCY AND THE SHORT-PERIOD FREQUENCY ON THE AIRPLANE DYNAMIC-RESPONSE FACTOR

By CARL R. HUSS and JAMES J. DONEGAN

Langley Research Center
Langley Field, Va.

TECHNICAL REPORT R–12

EFFECT OF THE PROXIMITY OF THE WING FIRST-BENDING FREQUENCY AND THE SHORT-PERIOD FREQUENCY ON THE AIRPLANE DYNAMIC-RESPONSE FACTOR [1]

By Carl R. Huss and James J. Donegan

SUMMARY

A study of the effect of the frequency of the lowest wing structural mode on the airplane center-of-gravity dynamic-response factor was made by employing simplified transfer functions. It was found that the simplified transfer function adequately predicted the maximum value of the incremental normal-load-factor response at the airplane center of gravity to isosceles triangle pulse elevator inputs.

The results of the study are presented in the form of preliminary design charts which give a comparison between the dynamic-response factors of the semirigid case and the airplane longitudinal short-period case and between the dynamic-response factors of the semirigid case and the steady-state value of the airplane longitudinal short-period response. These charts can be used to estimate the first-order effects of the addition of a wing-bending degree of freedom on the short-period dynamic-response factor and on the maximum dynamic-response factor when compared with the steady-state response of the system. The results show that a structurally damped frequency greater than six times the short-period damped frequency will not affect the dynamic-response factor of the semirigid short-period response at the airplane center of gravity and that, when the frequencies are equal, the semirigid dynamic-response factor may be as much as 1.6 times that of the short period. The results also show that the maximum dynamic-response factor can be as much as 2.4 times the steady-state response of the system, depending upon the ratio of the natural frequencies of the structural and short-period modes and upon the damping of the two modes.

INTRODUCTION

As airplanes have increased in size, speed, and flexibility, analysis of the loads, stresses, and deflections associated with the longitudinal short-period mode has become increasingly more complex. This complexity results from the need to include not only the aeroelastic effects associated with structural deformation but also the dynamic effects of structural vibration. Considerable effort is currently being expended in the field of dynamic analysis and it has become customary to express the dynamic effects of both aeroelasticity and structural vibration in terms of a dynamic-response factor which relates the dynamic response of the airplane to its steady-state response. The effects of flexibility are generally associated with a specific response at the center of gravity of the airplane, especially in the preliminary design stages; however, these effects at other points on the airframe (such as a wing-tip deflection or a strain in a particular structural member) are often of interest.

The present-day use of thin high-aspect-ratio wings on large high-speed airplanes has resulted in a lowering of the frequency of the wing structural vibratory modes. As a consequence of this reduction in stiffness, the frequency of the lowest wing vibratory mode is approaching the frequency of the airplane short-period mode. The proximity of the frequencies of these two modes has a pronounced effect on the airplane dynamic-response factor. Although this effect has been known qualitatively for some time and studies of specific configurations have been made, there has been no simple numerical guide for estimating the effects of this design trend. Possibly, this lack is a natural consequence of the nature of the mathematical transfer functions which relate the airplane center-of-gravity response to an incremental change in

[1] Supersedes NACA Technical Note 4250 by Carl R. Huss and James J. Donegan, 1958.

elevator angle. These transfer functions are of a type which is usually regarded as being more adaptable to specific studies than to generalization.

The purpose of this study was to determine whether the results obtained by using the complete transfer functions could also be obtained to a high degree of approximation with related but greatly simplified transfer functions and whether this simplification was of such a nature as to permit generalization of the results. The present paper illustrates the nature and validity of the simplification of the transfer function used and assesses as to both magnitude and trends the effect of the proximity of the frequencies of the lowest wing structural mode and the airplane short-period mode on the airplane incremental normal load factor at the airplane center of gravity. The results are summarized in the form of design charts which, it is believed, will be of value in the preliminary design stages of an airplane.

SYMBOLS

A_{Zh} generalized nondimensional mass-coupling term between Z and h degrees of freedom, $a_{Zh}/\rho S\bar{c}$

A_{hh} generalized nondimensional mass term of flexible-wing mode between elastic wing and h degree of freedom, $a_{hh}/\rho S\bar{c}$

$A_{\theta h}$ generalized nondimensional mass-coupling term between θ and h degrees of freedom, $a_{\theta h}/\rho S\bar{c}^2$

a_{Zh} generalized mass-coupling term between Z and h degrees of freedom, $2\int_0^{b_o/2}\{m'_w[f_z(y)]-S'_w f_\phi(y)\}dy_o$, slugs

a_{hh} generalized mass term of flexible-wing mode between elastic wing and h degree of freedom, $2\int_0^{b_o/2}\{m'_w[f_z(y)]^2 -2S'_w f_z(y)f_\phi(y)+I'_w[f_\phi(y)]^2\}dy_o$, slugs

$a_{\theta h}$ generalized mass-coupling term between θ and h degrees of freedom, $2\int_0^{b_o/2}[-S'_w f_z(y)+I'_w f_\phi(y) -m'_w l f_z(y)+S'_w l f_\phi(y)]dy_o$, slug-ft

b wing span along elastic axis, ft

$C_0, C_1, \ldots C_9$ dimensional transfer-function coefficients for semirigid case

$C'_1, C'_2, \ldots C'_9$ nondimensional transfer-function coefficients for semirigid case

C_F force coefficient due to elastic-wing deflection, F_h/qS

C_m airplane pitching-moment coefficient about the center of gravity, $M/qS\bar{c}$

C_N airplane normal-force coefficient at the airplane center of gravity, F_N/qS

$\bar{c}$ wing mean aerodynamic chord, ft

$D=\dfrac{d}{dt\frac{V}{\bar{c}}}$

E_K kinetic energy, ft-lb

E_p potential energy, ft-lb

F force, lb

F_N airplane normal force at center of gravity, positive downward, lb

$f_z(y)$ spanwise bending-mode shape along wing elastic axis

$f_\phi(y)$ spanwise twisting-mode shape about wing elastic axis per unit tip bending deflection, radians/ft

g acceleration due to gravity, ft/sec^2

H wing-tip deflection, $h/\bar{c}$, chords

h wing-tip deflection of elastic axis due to bending, positive downward, ft

I' section moment of inertia, $m'_w x^2$, slug-ft^2/ft

$K_0, K_1, K_2, K_7, K_8, K_9$ dimensional rigid transfer-function coefficients

$K'_1, K'_2, K'_7, K'_8, K'_9$ nondimensional rigid transfer-function coefficients

K_Y radius of gyration about Y-axis, chords

k reduced angular frequency, $\omega\bar{c}/V$

l longitudinal distance from airplane center of gravity to wing elastic axis (function of spanwise location), positive forward, ft

M pitching moment about center of gravity, ft-lb

m_A, m_f, m_w mass, slugs

m'_w section mass, slugs/ft

Δn	incremental normal load factor at airplane center of gravity (positive upward), g units
q	dynamic pressure, lb/sq ft; also, pitching angular velocity, radians/sec
S	wing plan-form area, sq ft
S'	section mass moment about elastic axis, $m'_w x$, slug-ft/ft
s	Laplace transform variable
T	period of oscillation, $\frac{2\pi}{\omega}$, sec
T_i	duration of triangular input, sec
t	time, sec
V	velocity, fps
x	longitudinal displacement, positive forward, ft
y	lateral or spanwise displacement, ft
Z	vertical displacement of airplane center of gravity, positive downward, ft
z	vertical wing deflection of elastic axis due to wing bending, positive downward, ft
α	angle of attack positive when wing leading edge is up, radians
$\Gamma_0, \Gamma_1, \ldots \Gamma_5$	dimensional quasi-steady transfer-function coefficients
$\Gamma'_1, \Gamma'_2, \ldots \Gamma'_5$	nondimensional quasi-steady transfer-function coefficients
γ	dynamic-response factor at airplane center of gravity, $(\Delta n_{dyn})_{max}/\Delta n_{static}$
$\Delta\delta_e$	incremental elevator deflection, positive when trailing edge is up, deg
θ	angle of pitch about airplane center of gravity, positive nose up, radians
Λ	sweep angle of elastic wing, deg
μ	nondimensional airplane mass, $m_A/\rho S\bar{c}$
ξ	damping parameter, percent of critical damping
ρ	mass density of air, slugs/cu ft
ϕ	angle of twist of airfoil in plane perpendicular to elastic axis, positive when wing leading edge is up, radians
ω	angular frequency, radians/sec

Subscripts:

A	airplane
d	damped
dyn	dynamic
f	fuselage; structural
h	flexible-wing degree of freedom
max	maximum
n	natural
o	exposed wing
sp	short period
sr	semirigid
w	wing
Z	vertical degree of freedom
θ	pitching degree of freedom

Dots are used to indicate differentiation with respect to time; for example, $\dot{\theta}=d\theta/dt$. The subscripts α, $\dot{\theta}$, $\dot{h}$, h, g, II, and δ indicate differentiation with respect to the subscripts; for example, $C_{N_\alpha}=dC_N/d\alpha$.

GENERAL CONSIDERATIONS

In the preliminary design stage of an airplane, the designer can, with presently available methods, estimate the longitudinal short-period dynamic-response characteristics of the center of gravity of a given configuration for rigid and quasi-steady airframes. The rigid airframe is defined in this paper as a structure that does not deform or vibrate, the quasi-steady airframe as one which can deform but not vibrate, and the semirigid airframe as one which can both deform and vibrate. The problem that the designer is faced with in this preliminary design stage is the effect of the airframe vibratory modes (particularly those of the wing since it is usually the most flexible) on the quasi-steady airframe longitudinal short-period dynamic response. The methods available for calculating these effects are usually rather complex or require information which would probably not be readily available at this stage of the design. The designer needs, therefore, some means of estimating these effects which are simple and are based on parameters which would be available.

In this paper such means are presented in the form of preliminary design charts which can be used to estimate the effects of the proximity of the frequencies of the lowest wing structural mode and the airplane short-period mode (quasi-steady case) on the dynamic response at the center of gravity of the semirigid airplane. The design charts are based on the philosophy that in the

preliminary design stage of a particular configuration the designer will be able to compute either the maximum incremental normal load factor for the quasi-steady case or the steady-state value of the incremental normal load factor of the quasi-steady case. The charts are restricted to estimating the effects of only the lowest vibratory wing bending mode on the incremental normal-load-factor response at the center of gravity to elevator control inputs. All other structural parts are considered rigid. The charts are further restricted to a comparison of dynamic-response factors which are defined as

$$\gamma=(\Delta n_{dyn})_{max}/\Delta n_{static} \tag{1}$$

where $(\Delta n_{dyn})_{max}$ is the maximum amplitude of the first peak of the time history of the incremental normal load factor at the center of gravity and Δn_{static} is the steady-state amplitude of the time history of incremental normal load factor.

METHOD OF ANALYSIS

The procedure followed in this paper for studying the effect of the proximity of the frequencies of the lowest structural wing mode and the short-period mode on the incremental normal-load dynamic-response factor at the airplane center of gravity was patterned after that of references 1 and 2. Dynamic systems representing the incremental normal-load-factor response at the center of gravity to an elevator input and defined mathematically by transfer functions were excited by various isosceles triangular inputs and the maximum values of the resulting time responses were expressed as ratios to the steady-state response factors. This procedure was followed for systems having the quasi-steady mode coupled with a structural mode (semirigid case) and for the quasi-steady mode alone for a wide range of configurations and frequencies and dampings of the two modes. The dynamic-response factors thus obtained for the system with two modes were then expressed as ratios to those obtained for the system with one mode to determine the effects in question.

Although triangular inputs were used in this study, it is believed that comparable results would be obtained for other shapes of pulse-type inputs since the process of expressing the semirigid results as ratios to the short-period results tend to eliminate the effects of different-shaped inputs. Isosceles triangle inputs were used in this paper for the following reasons: they approximate in shape severe pilot-imposed inputs; their frequency content could be easily varied by changing their duration T_i; their frequency content could be made sufficient to excite the wing structural mode; and they could be easily handled mathematically both by manual calculation and by automatic electronic calculation.

For existing airplanes with high-aspect-ratio, thin, flexible wings, the lowest structural frequency is usually associated with wing bending and, therefore, wing bending was selected as the lowest structural mode for this investigation. The theoretical system chosen for this study consisted of three degrees of freedom: freedom in pitch, vertical translation, and wing bending. The equations of motion developed by Lagrange's method describing this system have been previously established and are presented in reference 3. For convenience they are also restated in appendix A of this paper.

The assumptions made in this study included the following: linearity, no change in airplane forward velocity, small perturbations, and rigidity of the fuselage and tail assemblies. These assumptions may be summarized by the assumption that the motions of an aircraft with flexible wings are described by the equations given in appendix A. It was further assumed that the aircraft is statically and dynamically stable longitudinally, that is, that the aircraft short-period mode and structural mode are oscillatory and are damped.

As mentioned earlier in this section, the dynamic systems used in this paper were defined mathematically by transfer functions relating the incremental normal load factor at the center of gravity to an incremental elevator input. Some of the terms in the transfer functions could be eliminated with small loss in accuracy and the analysis was made by using these simplified transfer functions. In order to show this relationship, it is first necessary to define the complete transfer functions and then demonstrate the simplifications that can be made to obtain the simplified but practical transfer functions. Hereafter in this paper the word "complete" will refer to transfer functions containing all the terms and the word "simplified" will refer to the transfer function with some of its terms omitted.

COMPLETE TRANSFER FUNCTIONS

The complete transfer functions relating the incremental normal load factor at the center of gravity to the incremental elevator angle input for the semirigid case, the quasi-steady case, and the rigid case were obtained from the equations of motion given in appendix A.

Semirigid case.—The transfer function for the semirigid case which defines a system that has both wing quasi-steady deformation and wing vibration is, in nondimensional form,

$$\frac{\Delta n}{\Delta\delta_e}(s)=\frac{C'_5s^4+C'_6s^3+C'_7s^2+C'_8s+C'_9}{s^4+C'_1s^3+C'_2s^2+C'_3s+C'_4} \tag{2}$$

where the definitions of the C' coefficients are given in appendix B. In dimensional form the transfer function may be written as

$$\frac{\Delta n}{\Delta\delta_e}(s)=\frac{C_5s^4+C_6s^3+C_7s^2+C_8s+C_9}{s^4+C_1s^3+C_2s^2+C_3s+C_4} \tag{3}$$

where the conversion factors of C' to C are given in appendix C. The static value of this transfer function is seen to be C_9/C_4. The characteristic equation may be factored into two quadratic equations by Graeffe's method and written as

$$\frac{\Delta n}{\Delta\delta_e}(s)=\frac{C_5s^4+C_6s^3+C_7s^2+C_8s+C_9}{[s^2+2\xi_{sp}(\omega_n)_{sp}s+(\omega_n)_{sp}^2][s^2+2\xi_f(\omega_n)_fs+(\omega_n)_f^2]} \tag{4}$$

Quasi-steady case.—As indicated in reference 4 by letting rates of wing-tip deflection $D^2h=Dh=0$ in the equations for the semirigid case, the transfer function for the quasi-steady case may be formed. In this case the wings can deform but do not vibrate. The transfer function for the quasi-steady case may be written as

$$\frac{\Delta n}{\Delta\delta_e}(s)=\frac{\Gamma_3s^2+\Gamma_4s+\Gamma_5}{s^2+\Gamma_1s+\Gamma_2} \tag{5}$$

where the Γ coefficients are defined in appendixes B and C. The static value of this function is seen to be Γ_5/Γ_2. It is interesting to note that the static value of the semirigid case is equal to the static value of the quasi-steady case $C_9/C_4=\Gamma_5/\Gamma_2$, since $\Gamma_0\Gamma'_2=C_0C'_4$ and $\Gamma_0\Gamma'_5=C_0C'_9$.

Rigid case.—By letting $D^2h=Dh=h=0$ in the equation for the semirigid case, the transfer function for the rigid case may be formed and written as

$$\frac{\Delta n}{\Delta\delta_e}(s)=\frac{K_9s^2+K_8s+K_7}{s^2+K_1s+K_2} \tag{6}$$

where the K coefficients are defined in appendixes B and C. Although the transfer functions of the rigid case and the quasi-steady case have the same form, the transfer coefficients of the two cases differ in that the transfer coefficients of the rigid case are modified by the effects of wing deformation to give the quasi-steady-case transfer coefficients. The static value of this function is K_7/K_2.

SIMPLIFIED TRANSFER FUNCTIONS

In order to determine whether the number of terms in the complete transfer functions could be reduced, studies of 15 airplane configurations were made on an electronic analog computer by using the complete transfer functions for the semirigid case (eq. (4)) and the quasi-steady case (eq. (5)). The configurations used covered a range of wing sweep angles from 0° to 60°, of ratios of wing mass to airplane mass from 0.15 to 0.50, of airplane center-of-gravity positions from $0.25\bar{c}$ to $0.45\bar{c}$, and of dynamic pressures from 100 to 800 pounds per square foot. These studies indicated that some of the terms in the numerator of the transfer functions did not contribute appreciably to the maximum value of the time history of incremental normal load factor for triangular inputs but merely acted as phase shifters and thus were not required for the purposes of the present study. Typical results of these studies are shown for the semirigid case in figures 1 and 2 and for the quasi-steady case in figures 3 and 4.

Semirigid case.—The contribution of the numerator terms of the semirigid transfer function with each numerator coefficient equal to unity is shown in figure 1(a). In figure 1(b) the contribution of each of these same numerator terms is shown for typical values of the coefficients. From plots such as these it is seen that the C_9 term makes the most important contribution to the maximum value of the incremental normal load factor.

Calculations of incremental normal-load-factor time response to isosceles triangle inputs were then made by using only the C_9 term in the semirigid transfer function. These time histories were compared with time histories obtained from

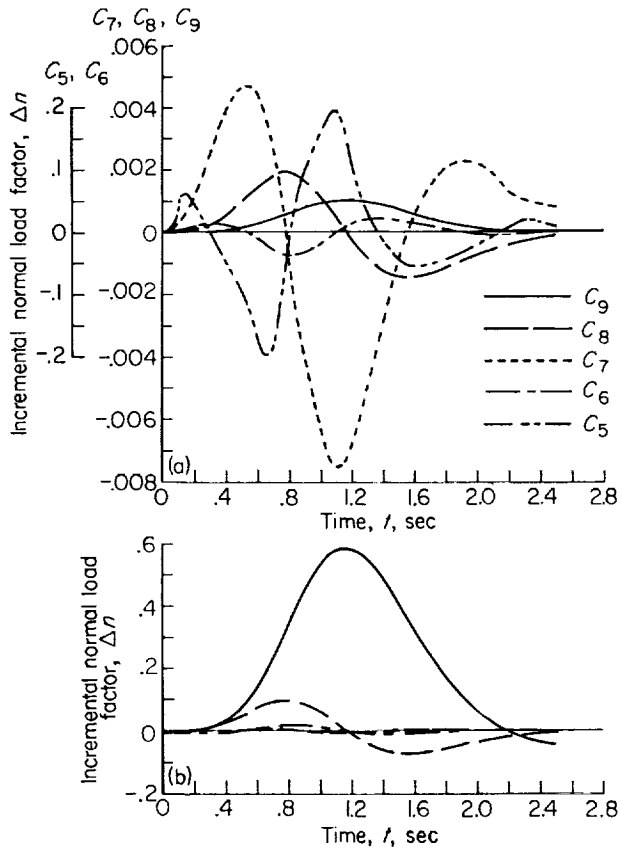

(a) Contribution of numerator terms with coefficients equal to unity.

(b) Contribution of numerator terms for typical values of the coefficients: $C_9=563.25$; $C_8=50.376$; $C_7=0.604$; $C_6=-0.504$; and $C_5=-0.0394$.

FIGURE 1. Contribution of individual numerator terms of the semirigid transfer function

$$\frac{\Delta n}{\Delta \delta_e}(s)=\frac{C_5 s^4+C_6 s^3+C_7 s^2+C_8 s+C_9}{s^4+C_1 s^3+C_2 s^2+C_3 s+C_4}$$

to the complete response to a unit-amplitude isosceles triangle input with $T_i=1.0$, $C_1=15.4414$, $C_2=116.8380$, $C_3=350.6639$, and $C_4=554.5269$.

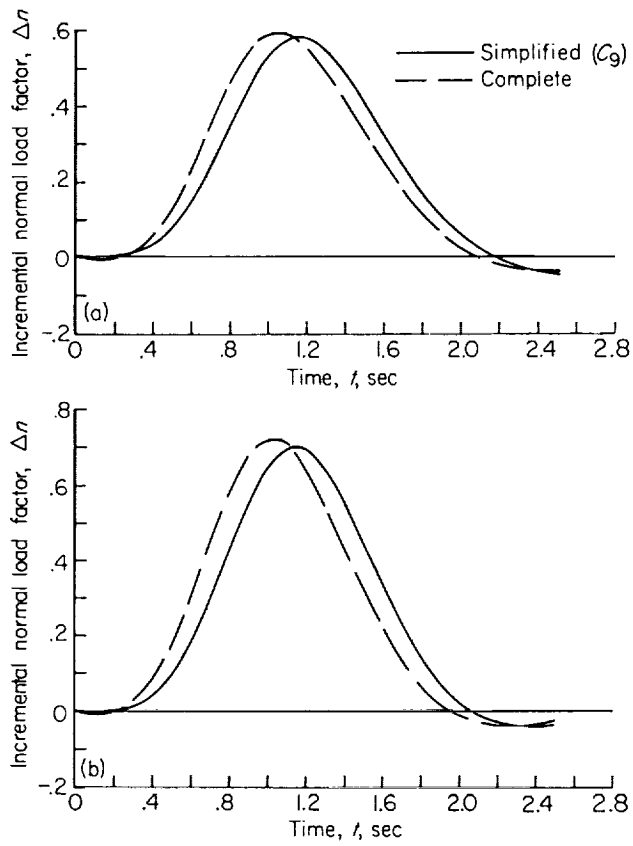

(a) Modes apart; $(\omega_d)_f/(\omega_d)_{sp}=2.44$.

(b) Modes together; $(\omega_d)_f/(\omega_d)_{sp}=1.0$.

FIGURE 2. Comparison of the response to a unit-amplitude isosceles triangle input with $T_i=1.0$ obtained from using the simplified semirigid transfer function

$$\frac{\Delta n}{\Delta \delta_e}(s)=\frac{C_9}{s^4+C_1 s^3+C_2 s^2+C_3 s+C_4}$$

and the complete semirigid transfer function

$$\frac{\Delta n}{\Delta \delta_e}(s)=\frac{C_5 s^4+C_6 s^3+C_7 s^2+C_8 s+C_9}{s^4+C_1 s^3+C_2 s^2+C_3 s+C_4}.$$

the complete transfer function (eq. (4)), to determine how well the simplified transfer function (C_9 term only in the numerator) described the maximum value of the time response of incremental normal load factor for triangular inputs. Typical comparisons are shown in figure 2(a) for the case when the frequencies of the modes are different and in figure 2(b) for the case when the frequencies of the modes are equal.

On the basis of such computations it was determined that the complete semirigid transfer function (eq. (4)) could be reduced to

$$\frac{\Delta n}{\Delta \delta_e}(s)=\frac{C_9}{[s^2+2\xi_{sp}(\omega_n)_{sp}s+(\omega_n)_{sp}^2][s^2+2\xi_f(\omega_n)_f s+(\omega_n)_f^2]} \tag{7}$$

and still adequately describe the maximum value of the time history of incremental normal load factor for triangular inputs. The use of the word "adequately" in this paper means generally to within about 3 percent and rarely more than about 10 to 15 percent.

Quasi-steady case.—A similar procedure was used to determine the contribution of the terms in

the numerator of the quasi-steady transfer function (eq. (5)) to the maximum value of the time response of the incremental normal load factor. In figure 3(a) the contribution of the numerator terms of the quasi-steady transfer function with each numerator coefficient equal to unity is shown. In figure 3(b) the contribution of each of these same numerator terms is shown for typical values of the coefficients. In this case it is seen that Γ_5 is the important term. Typical comparison of a time history obtained from the reduced transfer function (Γ_5 term only in the numerator) with that obtained from the complete transfer function (eq. (5)) is shown in figure 4.

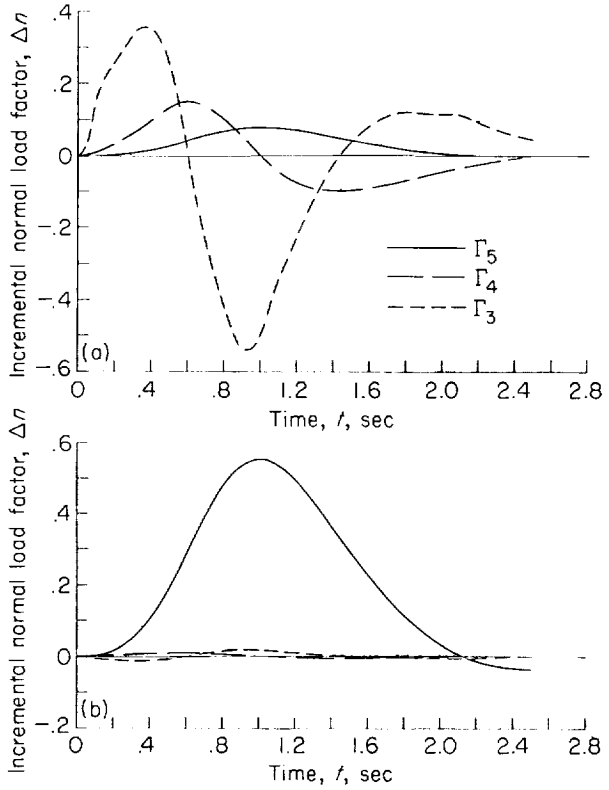

(a) Contribution of numerator terms with coefficients equal to unity.

(b) Contribution of numerator terms for typical values of the coefficients: $\Gamma_5=7.093$; $\Gamma_4=0.054$; and $\Gamma_3=-0.0355$.

FIGURE 3.—Contribution of individual numerator terms of the quasi-steady transfer function

$$\frac{\Delta n}{\Delta \delta_e}(s)=\frac{\Gamma_3 s^2+\Gamma_4 s+\Gamma_5}{s^2+\Gamma_1 s+\Gamma_2}$$

to the complete response to a unit-amplitude isosceles triangle input with $T_i=1.0$, $\Gamma_1=3.4328$, and $\Gamma_2=6.9934$.

From comparisons such as that shown in figure 4, it was determined that the complete quasi-steady transfer function (eq. (5)) could be reduced to

$$\frac{\Delta n}{\Delta \delta_e}(s)=\frac{\Gamma_5}{s^2+\Gamma_1 s+\Gamma_2} \tag{8}$$

and still adequately describe the maximum value of the time history of incremental normal load factor for triangular inputs.

Semirigid short-period case.—Since the denominator of equation (8) does not equal the short-period part of the denominator of equation (7), it was found convenient to define another transfer function. This transfer function will be called the semirigid short-period case and is defined as

$$\frac{\Delta n}{\Delta \delta_e}(s)=\frac{A}{s^2+2\xi_{sp}(\omega_n)_{sp}s+(\omega_n)_{sp}^2} \tag{9}$$

where the denominator of equation (9) is identical to the short-period part of the denominator of equation (7) and the constant A is equal to $\frac{C_9}{(\omega_n)_f^2}$.

The use of this semirigid short-period transfer function as a basis of comparison rather than the quasi-steady case reduced the computations to practical proportions. If the quasi-steady case had been used, it would have been necessary to estimate a new set of derivatives which make up

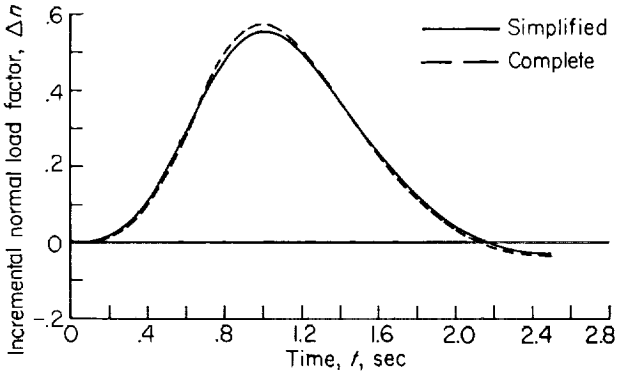

FIGURE 4.—Comparison of the response to a unit-amplitude isosceles triangle input with $T_i=1.0$ obtained from using the simplified quasi-steady transfer function

$$\frac{\Delta n}{\Delta \delta_e}(s)=\frac{\Gamma_5}{s^2+\Gamma_1 s+\Gamma_2}$$

and the complete quasi-steady transfer function

$$\frac{\Delta n}{\Delta \delta_e}(s)=\frac{\Gamma_3 s^2+\Gamma_4 s+\Gamma_5}{s^2+\Gamma_1 s+\Gamma_2}.$$

the transfer-function coefficients for each new configuration and flight condition. However, by defining the semirigid short period, it was necessary to choose only the damping and frequency of the two modes without regard to the derivatives which determine these parameters.

Actually, the semirigid short-period case is practically equal to the quasi-steady case since the damping and frequency of the two cases are almost the same for a wide range of configurations and q values. (See figs. 5 and 6.) A comparison of the natural frequencies of the semirigid short-period case with those of the quasi-steady case for a wide range of configurations and q values is shown in figure 5. A similar comparison of the damping of the semirigid short-period case with

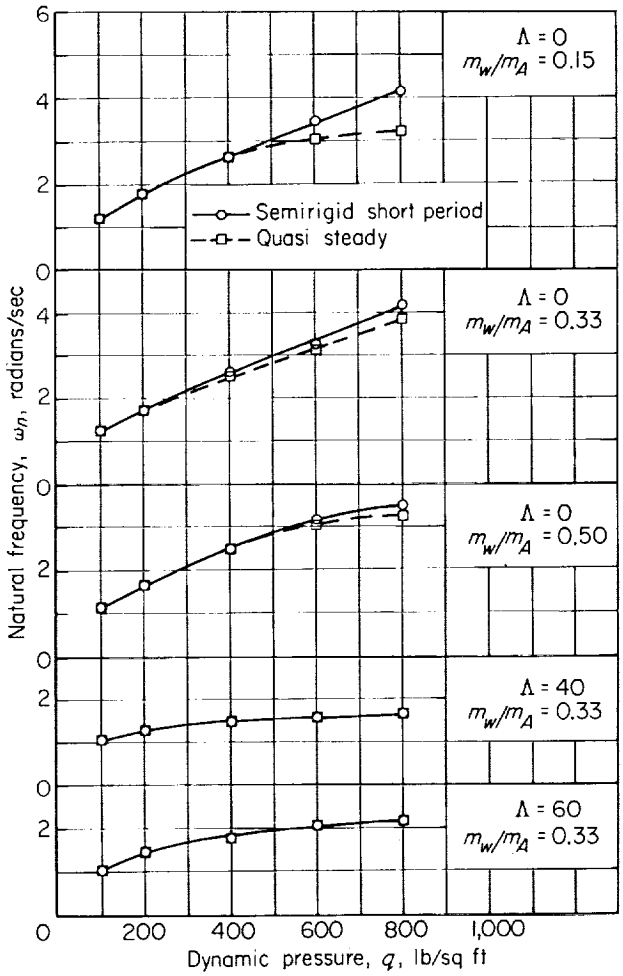

FIGURE 5.—Comparison of the natural frequency of the semirigid short-period mode with that of the quasi-steady mode at a center-of-gravity location of $0.25\bar{c}$.

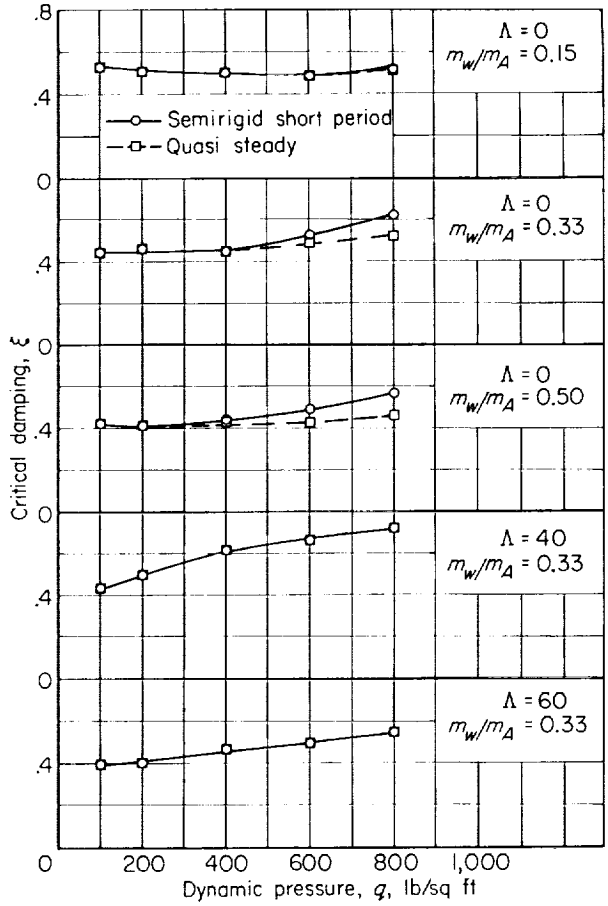

FIGURE 6.—Comparison of critical damping of the semirigid short-period mode with that of the quasi-steady mode at a center-of-gravity location of $0.25\bar{c}$.

that of the quasi-steady case is shown in figure 6. The points shown in figures 5 and 6 were computed from the data of reference 3. The data of figure 6 indicate that at the higher values of dynamic pressure the damping of the short-period case is greater than that of the quasi-steady case. Therefore the maximum value of the response as well as the maximum dynamic-response factor obtained from the short-period case would always be less than that of the quasi-steady case. Thus the ratios of maximum dynamic-response factors obtained by comparing the semirigid case with the short-period case would always be greater than (on the conservative side) or the same as those obtained by comparing the semirigid case with the quasi-steady case.

Rigid case.—The complete rigid transfer function (eq. (6)) could also be reduced to

$$\frac{\Delta n}{\Delta \delta_e}(s)=\frac{K_7}{s^2+K_1 s+K_2} \tag{10}$$

in order to define the maximum value of the time history of incremental normal load factor for triangular inputs.

TYPICAL CALCULATIONS ILLUSTRATING METHOD

The method used in this study and the preparation of the desired preliminary design charts involved a large number of calculations and plots, typical samples of which are shown in figures 7 and 8.

In order to obtain the maximum possible dynamic-response factor for the range of the variables, it was first necessary to calculate the time response to triangular inputs of varying duration (different frequency content) for each system (a particular combination of the variables). A sample of these calculations is shown in figure 7 for both the semirigid short-period and the semirigid cases. Some of these computations were carried out on automatic electronic computing equipment, some on desk-type computers, and some were carried out by using the tables of references 5 and 6 in conjunction with automatic electronic computing equipment. The dynamic-response factor defined previously as equation (1) was determined for each case by picking the value of the first peak of the time histories (see, for example, fig. 7 for $T_i=0.4$) and dividing it by the static value for the particular system being considered. These results were then plotted against the period ratio T_i/T_{sp} (ratio of the time base of the input to the natural period of the short-period mode) in order to determine the maximum dynamic-response factor for each case. A typical plot of this procedure is shown in figure 8. The

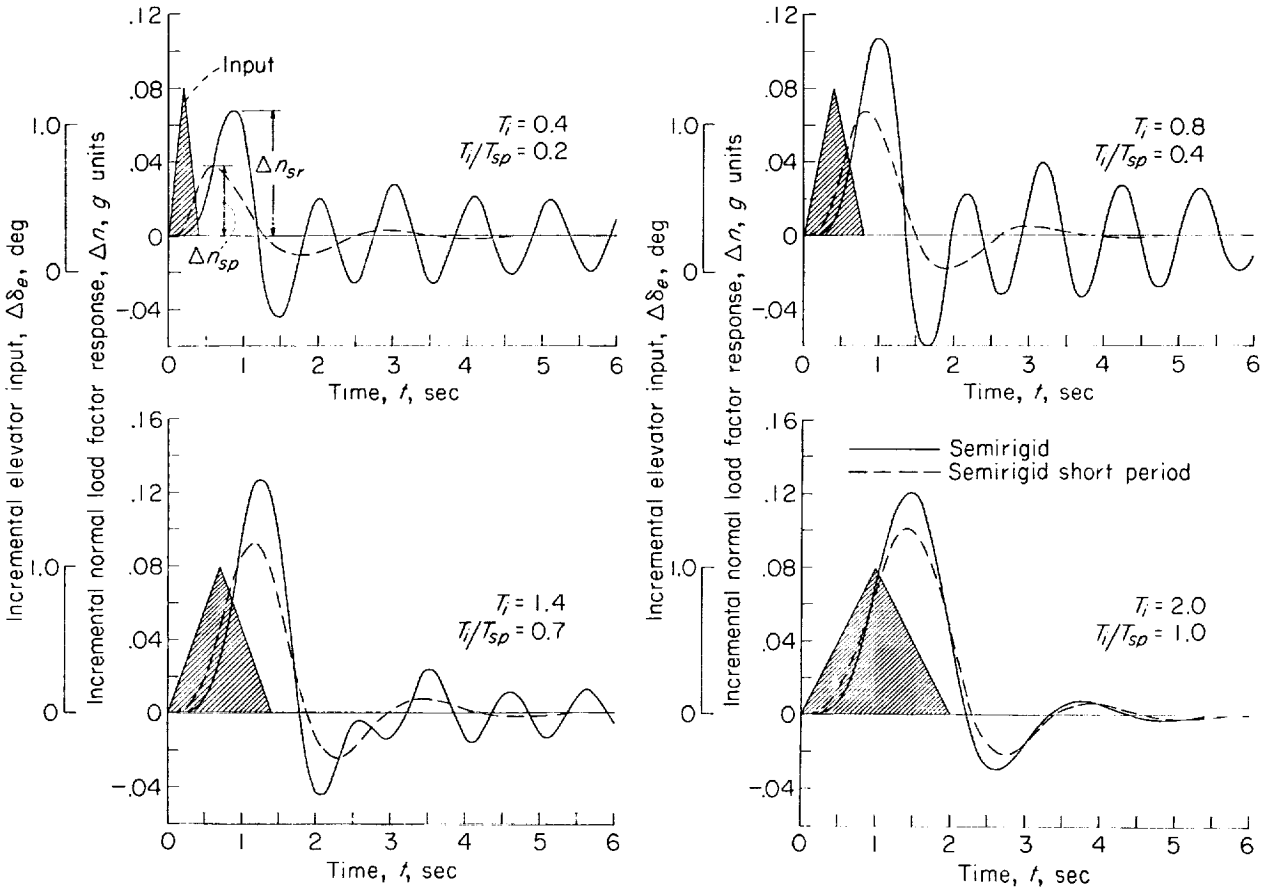

FIGURE 7.—Typical center-of-gravity incremental normal-load-factor time responses of the semirigid short-period and semirigid cases with a frequency ratio $(\omega_n)_f/(\omega_n)_{sp}$ of 1.9 to isosceles triangle inputs. $(\omega_n)_{sp}=3.162$; $\xi_{sp}=0.38$; $(\omega_n)_f=6.0$; $\xi_f=0.02$.

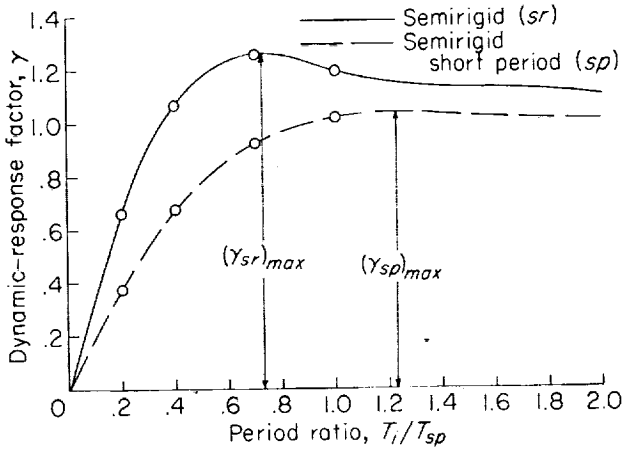

FIGURE 8.—Typical plot of dynamic-response factor γ against period ratio T_f/T_{sp} for the semirigid short-period case and semirigid case with a frequency ratio $(\omega_n)_f/(\omega_n)_{sp}$ of 1.9. $(\omega_n)_{sp}=3.162$; $\xi_{sp}=0.38$; $(\omega_n)_f=6.0$; $\xi_f=0.02$.

data of figure 8 are for the same cases as those of figure 7, the four points shown in figure 8 having been computed from the results shown in figure 7.

From plots such as that shown in figure 8, it was possible to ascertain the magnitude and trends of the effects of the proximity of the frequencies of the lowest structural mode and the airplane longitudinal short-period mode on the incremental normal-load dynamic-response factor at the airplane center of gravity. The plotting of these calculations resulted in the desired preliminary design charts.

RANGE OF VARIABLES

The results of this study are believed to be valid over a range of variables as follows: dynamic pressure from 100 to 800 pounds per square foot, wing sweep angles from 0° to 60°, ratios of wing mass to airplane mass of 0.15 to 0.50; center-of-gravity location from 0.25 to 0.45 mean aerodynamic chord, ratios of damped wing lowest structural frequency to damped airplane longitudinal short-period frequency from 1 to 15, and damping of the wing lowest structural mode and airplane longitudinal short-period mode from 0 to 95 percent of critical damping.

RESULTS AND DISCUSSION

The results of this paper are summarized in the form of preliminary design charts. As mentioned previously, these design charts were obtained from plots such as those of figure 8 covering a complete range of combinations of the variables.

The chart given as figure 9 is a plot of the ratios of maximum dynamic-response factors $(\gamma_{sr})_{max}/(\gamma_{sp})_{max}$ against the ratio of the structural-mode natural frequency divided by the semirigid short-period natural frequency, the damping of the structural mode being held constant at 2 percent of critical damping. The data of figure 9 were reduced to a more compact form by converting the abscissa to a ratio of the damped frequency of the structural mode and the damped semirigid short-period frequency. This simplification is given as the design chart shown in figure 10.

The design chart shown in figure 10 indicates that, if the damped structural frequency and the damped semirigid short-period frequency are equal, the maximum dynamic-response factor of the semirigid case will be about 1.6 times the value of the maximum dynamic-response factor for the semirigid short-period case. It can also be seen that, when the ratio of the damped structural frequency and the damped semirigid short-period frequency is greater than about 6, there is no increase in the maximum dynamic-response factor of the semirigid case over the value for the semirigid short-period case.

Increasing the damping of the short-period mode of the semirigid case while holding the damping of the structural mode constant also results in a decrease in the maximum dynamic-response factor of the semirigid case. This effect can be seen from the results shown in figure 9.

In order to investigate the effect of structural damping on the airplane dynamic-response factor, calculations were made for a semirigid short-period mode with a natural frequency of 3.162 radians per second and a damping of 38 percent of critical damping coupled to a structural mode having variable damping of 0 to 95 percent of critical damping and a damped frequency equal to the semirigid short-period damped frequency (2.926 radians per second) and equal to 5 times the semirigid short-period damped frequency. Dynamic-response-factor ratios for these cases are plotted against critical damping of the structural mode in figure 11. The result shown in figure 11 indicates that, for a given value of damping of the short-period part of the semirigid case, an increase in the damping of the structural mode results in a decrease in the maximum dynamic-response factor of the semirigid case.

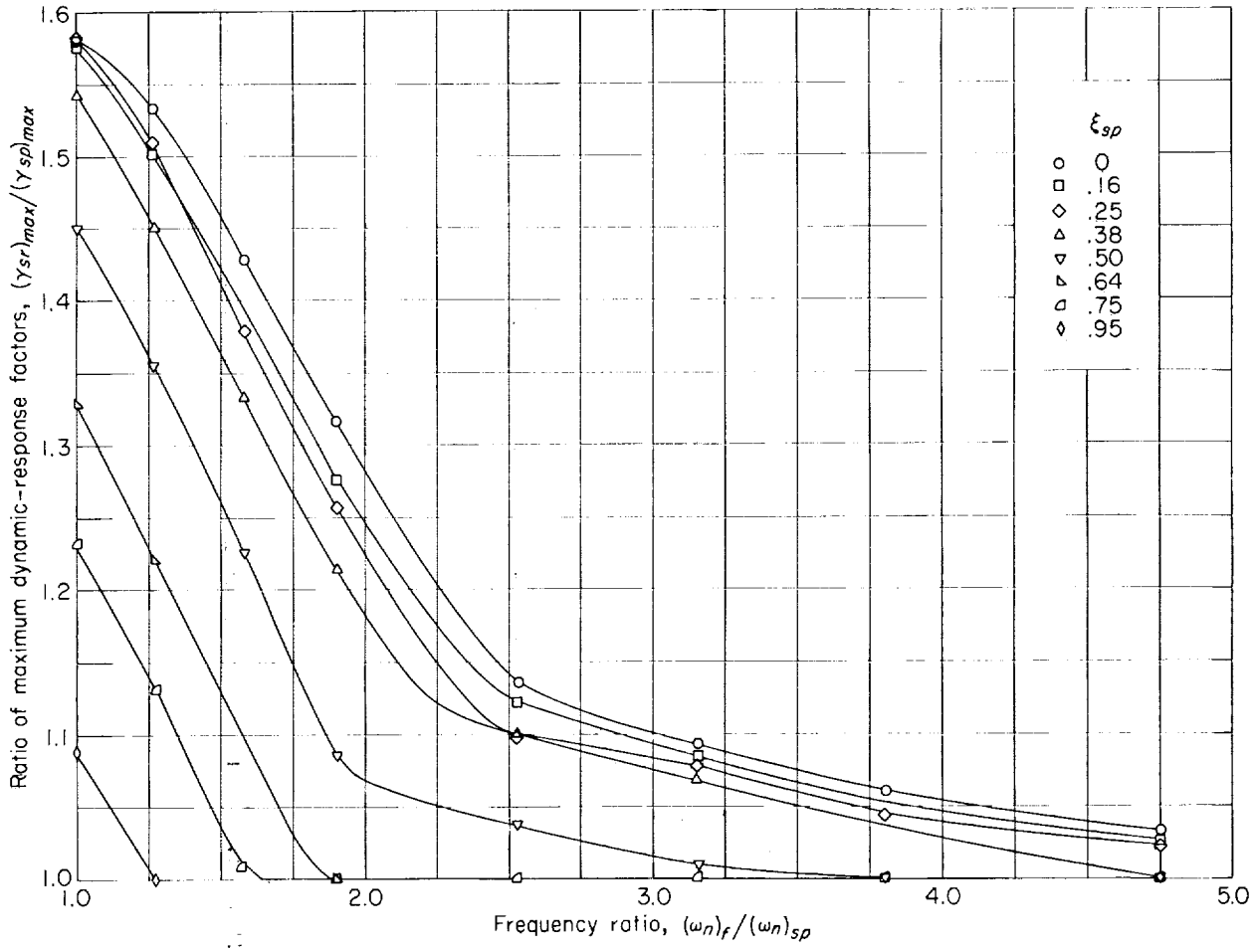

FIGURE 9.—Effect on the ratio of maximum dynamic-response factors of the proximity of the structural natural frequency to the semirigid short-period natural frequency. $\xi_f=0.02$.

Thus, the data of figures 9, 10, and 11 indicate that, for a given frequency of the short-period mode of the semirigid case, an increase in the frequency and/or an increase in damping of the structural mode and/or an increase in damping of the semirigid short-period mode result in a decrease of the maximum dynamic-response factor of the semirigid case. Figures 9, 10, and 11 would be the ones used by a designer in order to obtain an estimate of the increase in the incremental normal-load short-period dynamic-response factor at the airplane center of gravity due to the proximity of the frequency of the lowest wing structural mode to that of the airplane longitudinal short-period mode. Use of these figures presumes, as mentioned earlier, that the designer would be able to estimate the maximum longitudinal short-period response and would have an estimate of the lowest wing structural frequency and damping of the lowest wing structural mode.

Another design figure which may be useful is one which gives the effect of the proximity of the structural natural frequency to the short-period natural frequency on the maximum semirigid dynamic response when compared with the semirigid short-period static value. This result was easily obtained by plotting the semirigid maximum dynamic-response factor for each case (obtained from plots such as fig. 8 and noting that, as pointed out earlier, the static value of the semirigid and semirigid short-period cases are equal) against the ratio of the structural natural frequency to the semirigid short-period natural frequency. Such a plot is presented as figure 12.

The designer could use the chart given in figure 12 under the same restrictions as were mentioned

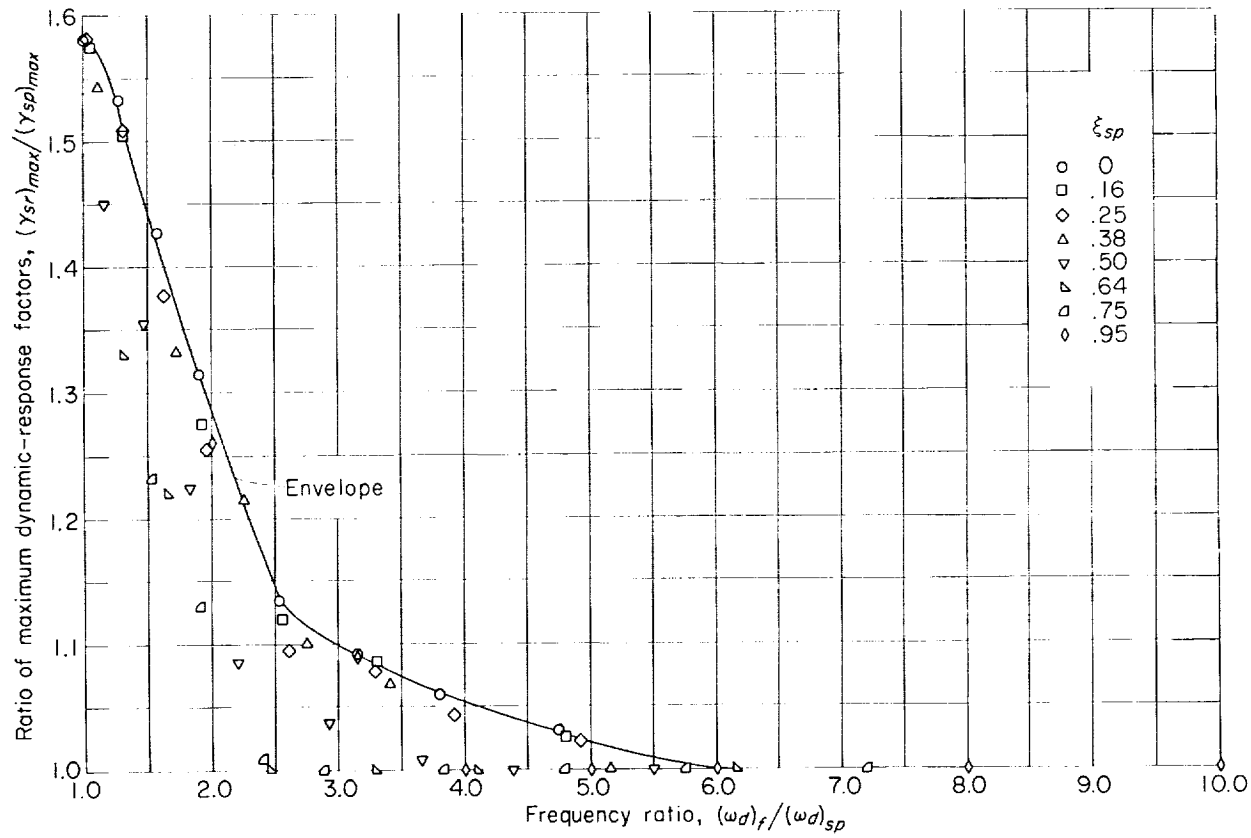

FIGURE 10.—Effect on the ratio of maximum dynamic-response factors of the proximity of the structural damped frequency to the semirigid short-period damped frequency. $\xi_f = 0.02$.

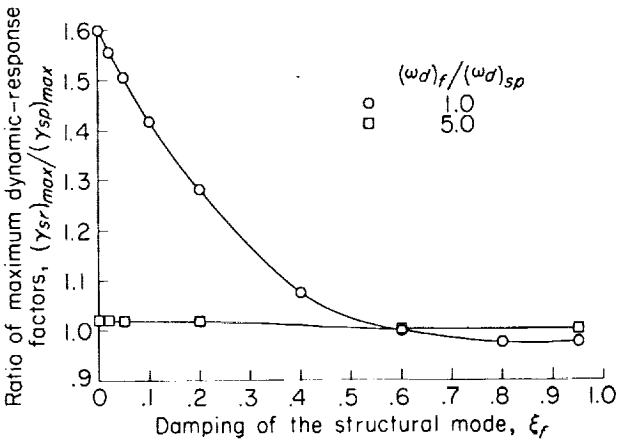

FIGURE 11.—Effect of damping of the structural mode on the ratio of maximum dynamic-response factors for two ratios of the damped structural and semirigid short-period frequencies for semirigid short-period damping of 0.38.

for the previous charts with one exception. This exception is that in using this chart the designer would need to know only the airplane longitudinal short-period steady-state response rather than the maximum short-period response.

The effect of the input-time base on the dynamic-response-factor ratio may also be of interest and can be determined from plots such as that of figure 8. In this case, rather than express the maximum values of the dynamic-response factor as ratios, the values of the dynamic-response factor of the semirigid and short-period frequencies are expressed as ratios at specific values of the period ratio T_i/T_{sp} and are plotted against the period ratio. Typical plots of this dynamic-response-factor ratio are shown in figure 13 for three values of short-period damping.

The base of the input that gives the maximum dynamic-response factor is, of course, different for each case, depending on the damping of the two modes. It was usually greater than about 0.7 of the natural period of the short period for all the cases studied in this paper. Examination of plots, such as those shown in figure 13, indicate that, when compared for the same triangle base, the

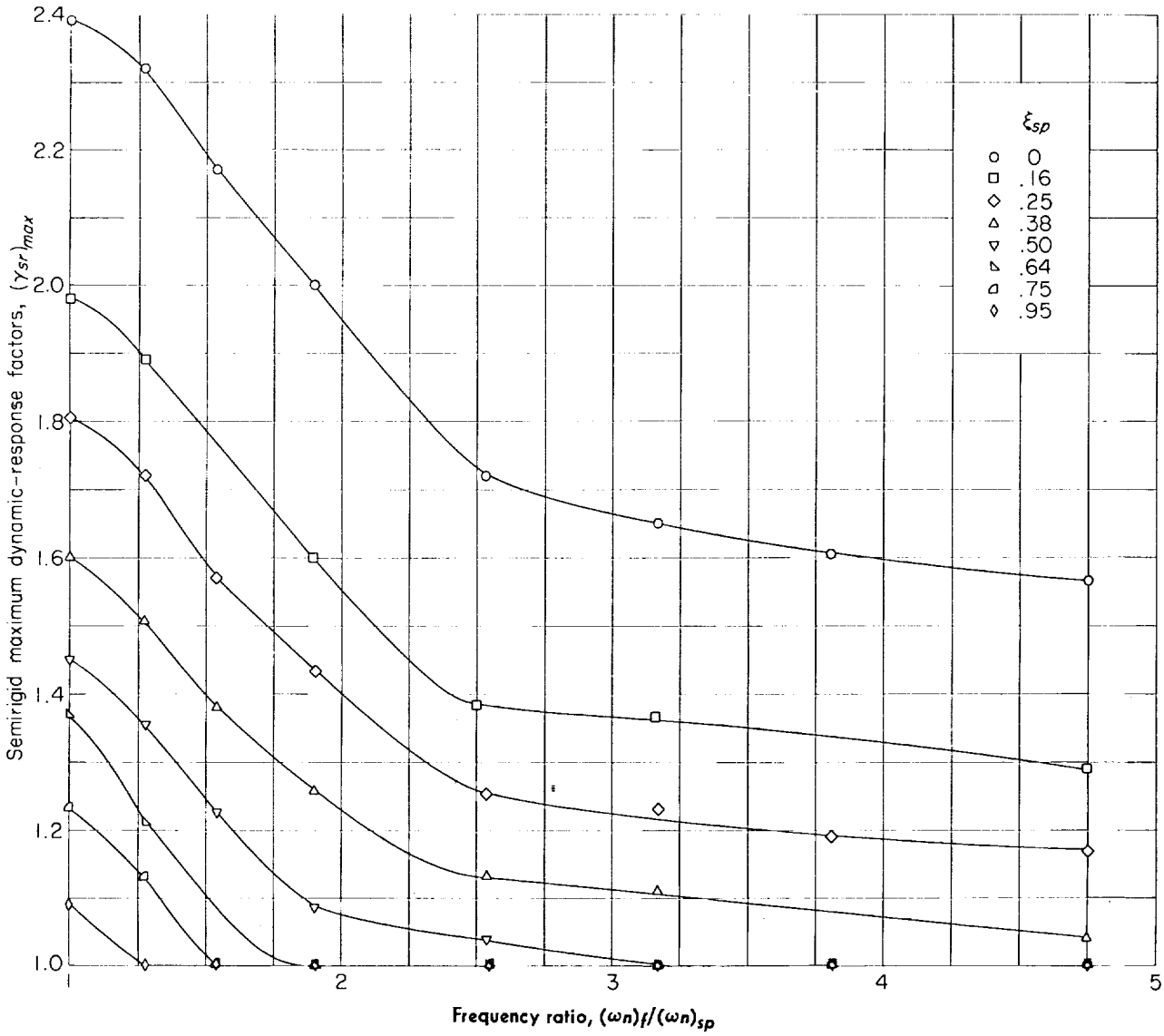

FIGURE 12.—Effect of the proximity of the structural natural frequency to the semirigid short-period natural frequency on the semirigid maximum dynamic-response factor. $\xi_f=0.02$.

highest ratio of dynamic-response factor for a frequency ratio of 1.0 will be obtained from triangular inputs with a base equal to 0.6 to 0.8 of the natural period of the short period. For frequency ratios greater than 1.0, the ratio of dynamic-response factors is greatest for triangles with a base equal to less than 0.1 of the natural period of the short period. Thus, it is difficult to pinpoint a specific triangle base as being the one giving the most severe results.

Since airplanes operate at flight conditions (altitude, airspeed, center-of-gravity location) which are constantly changing, the frequency ratio for a particular configuration will not be constant. Present-day large high-speed airplanes with thin, high-aspect-ratio, flexible wings are operating in the frequency-ratio range of roughly 4 to 10. The conditions for which the frequency ratio will be a minimum depends somewhat on the configuration but, in general, operations at low altitude, high airspeed, and forward center-of-gravity position should result in the lowest frequency ratio. This effect can be seen in figure 14 where the effect of dynamic pressure and airplane configuration on the proximity of the damped frequency of the structural mode to that of the short-period mode

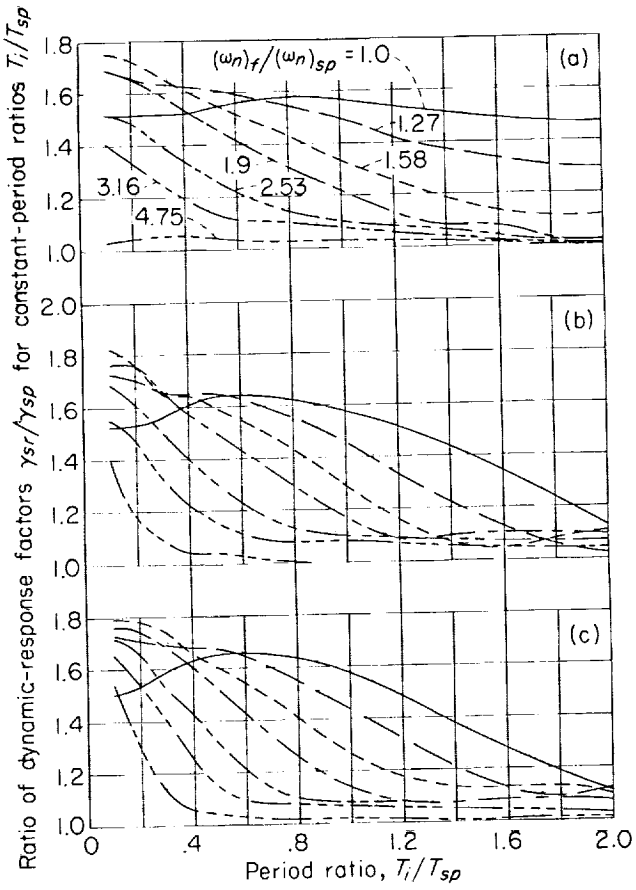

(a) $\xi_{sp}=0$; $\xi_f=0.02$.

(b) $\xi_{sp}=0.38$; $\xi_f=0.02$.

(c) $\xi_{sp}=0.95$; $\xi_f=0.02$.

FIGURE 13.—Typical plots of the effect of the period ratio on the ratio of dynamic-response factors for various frequency ratios.

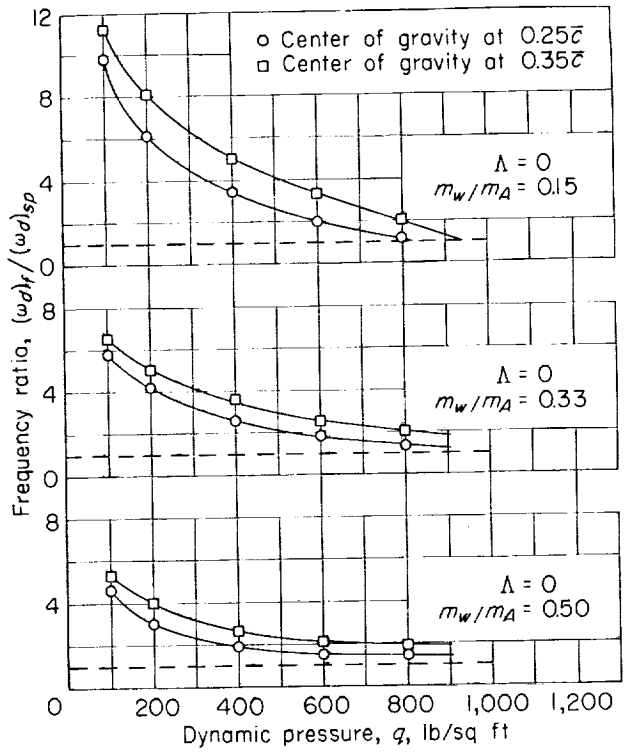

FIGURE 14.—Effect of dynamic pressure q on the frequency ratio $(\omega_d)_f/(\omega_d)_{sp}$ for various wing sweep angles, wing-mass-to-airplane-mass ratios, and center-of-gravity locations.

is given. The data of this figure were converted from the data of reference 3.

The data of figure 14 show that, for airplanes with unswept wings or wings with very little sweep, the frequencies of the modes are brought into closer proximity by an increase in the dynamic pressure or, for a given dynamic pressure, by moving the center of gravity forward. For wings with sweep angles greater than about 30°, these trends of the effects of dynamic pressure and center-of-gravity position on the proximity of the frequencies of the modes are the same. For these cases, however, the aeroelastic effects caused by increasing the dynamic pressure usually cause the short-period mode to become statically unstable (indicated in fig. 14 by the frequency ratio going to infinity) before the frequencies of the modes can be brought together. Thus, for a given configuration the operating conditions will determine the relative proximity of the frequencies of the two modes and at what point on the abscissas of the design charts the airplane is operating.

It is well to emphasize that the preliminary design charts given are only meant to give first-order effects and to apply only to systems which are statically and dynamically stable. Furthermore, since the curve given in figure 10 is an envelope of the maximum values of the converted data of figure 9, it will normally give conservative values of the ratio of maximum dynamic-response factors. Finaliy, for a particular design problem a detailed analysis including all the variables should be made if the "rule-of-thumb" value for the ratio of maximum dynamic-response factors given by the chart indicates the possibility of a dangerous situation.

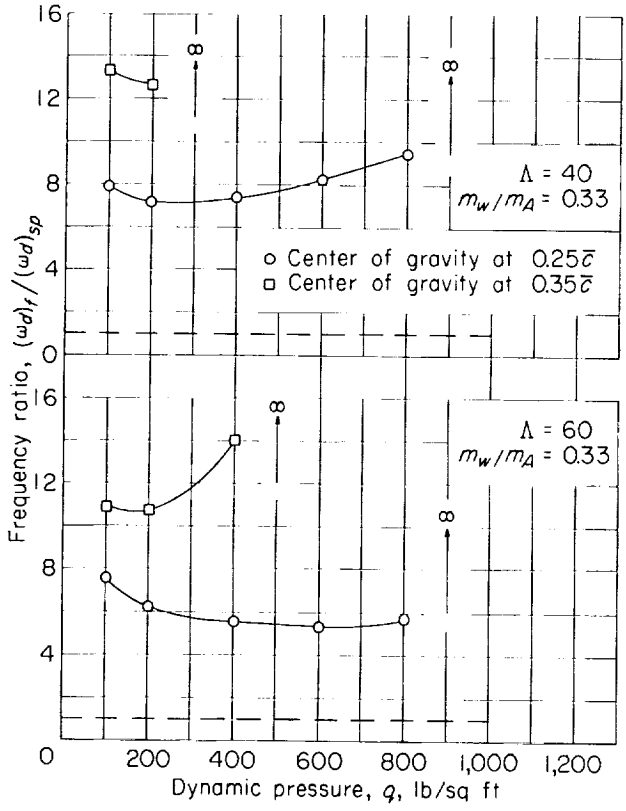

FIGURE 14.—Concluded.

CONCLUDING REMARKS

The results of this study of the effect of the frequency of the first wing bending mode on the airplane dynamic-response factor indicated that the maximum center-of-gravity load-factor response to a triangular-shaped pulse elevator input could be adequately determined by using a simplified transfer function for the semirigid and quasi-static cases. The use of the short-period part of the semirigid transfer function as a basis of comparison gave results which were either equal to or on the conservative side of those that would have been obtained from the quasi-steady transfer function.

As a result of the reduction in the number of terms obtained by using the simplified transfer functions, it was possible to construct design charts which provide trends and rule-of-thumb estimates of the effect of the frequency of the first wing-bending mode on the airplane dynamic-response factor. The charts show that the maximum dynamic-response factor for the semirigid case will be 1.6 times that of the short-period case when the damped frequencies of the structural mode and short-period mode are equal. Furthermore, when the frequency ratio is greater than about 6, a lightly damped structural mode has little or no effect on the dynamic-response-factor ratio at the airplane center of gravity, and, as the damping of the structural mode increases, the frequency ratio at which the structural mode has negligible effect also decreases. Finally, the charts indicate that the semirigid maximum dynamic-response factor can be as much as 2.4 times the steady-state value of the system, depending on the damping of the structural and short-period modes and on the ratio of the natural frequencies of the two modes.

The dynamic-response factor for a particular configuration will vary with the operating conditions (principally with dynamic pressure) but should be a maximum at flight conditions of low altitude, high airspeed, and forward center-of-gravity position.

It should be repeated that for a particular design problem a detailed analysis should be made if the rule-of-thumb value given by the design charts indicates the possibility of a dangerous situation.

LANGLEY RESEARCH CENTER,
NATIONAL AERONAUTICS AND SPACE ADMINISTRATION,
LANGLEY FIELD, VA., *February 21, 1958.*

APPENDIX A

EQUATIONS OF MOTION

The equations of motion used in this paper will be given here briefly for the convenience of the reader. A complete development of these equations is shown in references 3 and 4. The equations are derived on the basis of the Lagrangian equation:

$$\frac{d}{dt}\left(\frac{\partial E_k}{\partial Q}\right)-\frac{\partial E_k}{\partial Q}+\frac{\partial E_p}{\partial Q}=F_Q \tag{A1}$$

where

E_k kinetic energy
E_p potential energy
Q generalized coordinate
F_Q generalized force

The three generalized coordinates used are:

Z vertical translation
θ pitching velocity
h displacement of wing tip due to bending of elastic wing

For an unswept wing the flexible-wing mode shape consists of bending $f_z(y)$; and for a swept wing the flexible-wing mode shape consists of bending $f_z(y)$ combined with twisting per unit bending deflection at the wing tip $f_\phi(y)$. The spanwise bending is usually assumed to be parabolic and the spanwise twist, linear.

The nondimensional equations of motion thus derived are:

$$2\mu D(\alpha-\theta)+2A_{Zh}D^2H-C_{N_\alpha}\alpha-D\alpha\left(\frac{1}{2}C_{N_{D\alpha}}\right)-D\theta\left(\frac{1}{2}C_{N_q}\right)-H(C_{N_H})-DH(C_{N_{DH}})=C_{N_{\Delta\delta_e}}\Delta\delta_e \tag{A2}$$

$$2\mu K_Y{}^2D^2\theta+2A_{\theta h}D^2H-C_{m_\alpha}\alpha-D\alpha\left(\frac{1}{2}C_{m_{D\alpha}}\right)-D\theta\left(\frac{1}{2}C_{m_q}\right)-H(C_{m_H})-DH(C_{m_{DH}})=C_{m_{\Delta\delta_e}}\Delta\delta_e \tag{A3}$$

$$2A_{hh}D^2H+2A_{Zh}D(\alpha-\theta)+2A_{\theta h}D^2\theta+2A_{hh}k^2H-C_{F_\alpha}\alpha-D\theta\left(\frac{1}{2}C_{F_q}\right)-H(C_{F_H})-DH(C_{F_{DH}})-C_{F_{\Delta\delta_e}}\Delta\delta_e \tag{A4}$$

and by definition

$$\frac{\Delta n}{\Delta\delta_e}=\frac{V}{g}\left(\frac{D\theta}{\Delta\delta_e}-\frac{D\alpha}{\Delta\delta_e}\right) \tag{A5}$$

Simultaneous solution of equations (A2), (A3), (A4), and (A5) results in the semirigid transfer function given as equation (3).

APPENDIX B

DEFINITION OF TRANSFER-FUNCTION COEFFICIENTS

The transfer coefficients used for the analysis are defined in this appendix.

SEMIRIGID CASE

The coefficients for the semirigid case are

$$C_0=4(\mu K_Y^2 A_{hh}-A_{\theta h}^2)\left(2\mu-\frac{1}{2}C_{N_{D\alpha}}\right)-2(A_{\theta h}A_{Zh}C_{m_{D\alpha}}+4\mu K_Y^2 A_{Zh}^2)$$

$$C'_1=\frac{1}{C_0}\Bigg\{4\mu K_Y^2[A_{Zh}(C_{F_\alpha}+C_{N_{DH}})-A_{hh}C_{N_\alpha}]-(A_{hh}C_{m_q}+2\mu K_Y^2 C_{F_{DH}}-2A_{\theta h}C_{m_{DH}})\left(2\mu-\frac{1}{2}C_{N_{D\alpha}}\right)$$
$$+(4A_{\theta h}A_{Zh}+A_{hh}C_{m_{D\alpha}})\left(-2\mu-\frac{1}{2}C_{N_q}\right)+\left[A_{Zh}C_{m_{D\alpha}}+2A_{\theta h}\left(2\mu-\frac{1}{2}C_{N_{D\alpha}}\right)\right]\left(2A_{Zh}+\frac{1}{2}C_{F_q}\right)$$
$$+4A_{\theta h}(A_{\theta h}C_{N_\alpha}-A_{Zh}C_{m_\alpha})+A_{\theta h}C_{m_{D\alpha}}C_{N_{DH}}+2A_{Zh}^2C_{m_q}\Bigg\}$$

$$C'_2=\frac{1}{C_0}\Bigg\{4\mu K_Y^2 A_{hh}\left(2\mu-\frac{1}{2}C_{N_{D\alpha}}\right)k^2+2\mu K_Y^2(C_{N_\alpha}C_{F_{DH}}-C_{F_\alpha}C_{N_{DH}}+2A_{Zh}C_{NH})+\left(\frac{1}{2}C_{m_q}C_{F_{DH}}$$
$$-2\mu K_Y^2 C_{F_H}+2A_{\theta h}C_{m_H}\right)\left(2\mu-\frac{1}{2}C_{N_{D\alpha}}\right)+\left(2A_{Zh}C_{m_\alpha}-2A_{\theta h}C_{N_\alpha}-\frac{1}{2}C_{N_{DH}}C_{m_{D\alpha}}\right)\left(2A_{Zh}+\frac{1}{2}C_{F_q}\right)$$
$$+\left(2A_{hh}C_{m_\alpha}-2A_{\theta h}C_{F_\alpha}-2A_{Zh}C_{m_{DH}}-\frac{1}{2}C_{F_{DH}}C_{m_{D\alpha}}\right)\left(-2\mu-\frac{1}{2}C_{N_q}\right)+C_{m_q}[A_{hh}C_{N_\alpha}-A_{Zh}(C_{F_\alpha}$$
$$+C_{N_{DH}})]+2A_{\theta h}\left(C_{m_\alpha}C_{N_{DH}}-C_{N_\alpha}C_{m_{DH}}+\frac{1}{2}C_{NH}C_{m_{D\alpha}}\right)-C_{m_{DH}}\left(2\mu-\frac{1}{2}C_{N_{D\alpha}}\right)\left(2A_{Zh}+\frac{1}{2}C_{F_q}\right)\Bigg\}$$

$$C'_3=\frac{1}{C_0}\Bigg\{\left[-4\mu K_Y^2 C_{N_\alpha}-C_{m_q}\left(2\mu-\frac{1}{2}C_{N_{D\alpha}}\right)+C_{m_{D\alpha}}\left(-2\mu-\frac{1}{2}C_{N_q}\right)\right]A_{hh}k^2+2\mu K_Y^2(C_{N_\alpha}C_{F_H}$$
$$-C_{F_\alpha}C_{N_H})+2A_{\theta h}(C_{m_\alpha}C_{N_H}-C_{N_\alpha}C_{m_H})+\left[\frac{1}{2}C_{m_q}C_{F_H}-C_{m_H}\left(2A_{Zh}+\frac{1}{2}C_{F_q}\right)\right]\left(2\mu-\frac{1}{2}C_{N_{D\alpha}}\right)$$
$$-\left(C_{m_\alpha}C_{N_{DH}}+\frac{1}{2}C_{m_{D\alpha}}C_{N_H}-C_{N_\alpha}C_{m_{DH}}\right)\left(2A_{Zh}+\frac{1}{2}C_{F_q}\right)+\left(C_{F_\alpha}C_{m_{DH}}-2C_{m_H}A_{Zh}-C_{m_\alpha}C_{F_{DH}}\right.$$
$$\left.-\frac{1}{2}C_{m_{D\alpha}}C_{F_H}\right)\left(-2\mu-\frac{1}{2}C_{N_q}\right)+(C_{F_\alpha}C_{N_{DH}}-C_{N_\alpha}C_{F_{DH}}-2A_{Zh}C_{N_H})\frac{1}{2}C_{m_q}\Bigg\}$$

$$C'_4=\frac{1}{C_0}\Bigg\{\left[\frac{1}{2}C_{N_\alpha}C_{m_q}+C_{m_\alpha}\left(-2\mu-\frac{1}{2}C_{N_q}\right)\right](2A_{hh}k^2-C_{F_H})+(C_{N_\alpha}C_{m_H}$$
$$-C_{m_\alpha}C_{N_H})\left(2A_{Zh}+\frac{1}{2}C_{F_q}\right)+\left[C_{F_\alpha}C_{m_H}\left(-2\mu-\frac{1}{2}C_{N_q}\right)\right]+\frac{1}{2}C_{m_q}C_{F_\alpha}C_{N_H}\Bigg\}$$

$$C'_5=\frac{V}{gC_0}(4A_{\theta h}^2C_{N_\delta}-4A_{Zh}A_{\theta h}C_{m_\delta}-4\mu K_Y^2 A_{hh}C_{N_\delta})$$

$$C'_6=\frac{V}{gC_0}\Big[A_{hh}C_{N_\delta}(C_{m_{D\alpha}}+C_{m_q})-A_{hh}C_{m_\delta}(C_{N_{D\alpha}}+C_{N_q})+2A_{\theta h}C_{N_\delta}(2A_{Zh}-C_{m_{DH}})+2(A_{Zh}C_{m_\delta}$$
$$-A_{\theta h}C_{N_\delta})\left(2A_{Zh}+\frac{1}{2}C_{F_q}\right)+2C_{m_\delta}(A_{\theta h}C_{N_{DH}}-2A_{Zh}^2)+2\mu K_Y^2 C_{F_{DH}}C_{N_\delta}\Big]$$

$$C'_7=\frac{V}{gC_0}\Big[-4\mu K_Y{}^2C_{N_\delta}A_{hh}k^2+2A_{Zh}C_{m_\delta}(C_{N_{DH}}+C_{F_\alpha})+2A_{hh}(C_{m_\alpha}C_{N_\delta}-C_{N_\alpha}C_{m_\delta})+2A_{\theta h}(C_{N_H}C_{m_\delta}-C_{F_\alpha}C_{N_\delta})$$
$$+(C_{m_{DH}}C_{N_\delta}-C_{N_{DH}}C_{m_\delta})\Big(2A_{Zh}+\frac{1}{2}C_{F_q}\Big)+\frac{1}{2}C_{F_{DH}}C_{m_\delta}(C_{N_{D\alpha}}+C_{N_q})$$
$$-\frac{1}{2}C_{F_{DH}}C_{N_\delta}(C_{m_{D\alpha}}+C_{m_q})+2C_{N_\delta}(\mu K_Y{}^2C_{F_H}-A_{Zh}C_{m_{DH}}-A_{\theta h}C_{m_H})\Big]$$

$$C'_8=\frac{V}{gC_0}\Big\{A_{hh}k^2C_{N_\delta}(C_{m_{D\alpha}}+C_{m_q})-A_{hh}k^2C_{m_\delta}(C_{N_{D\alpha}}+C_{N_q})+C_{m_\delta}\Big[C_{N_\alpha}C_{F_{DH}}-C_{F_\alpha}C_{N_{DH}}$$
$$+\frac{1}{2}C_{F_H}(C_{N_{D\alpha}}+C_{N_q})\Big]+C_{N_\delta}\Big[C_{F_\alpha}C_{m_{DH}}-C_{m_\alpha}C_{F_{DH}}-\frac{1}{2}C_{F_H}(C_{m_{D\alpha}}+C_{m_q})\Big]$$
$$+2A_{Zh}(C_{N_H}C_{m_\delta}-C_{m_H}C_{N_\delta})+(C_{m_H}C_{N_\delta}-C_{N_H}C_{m_\delta})\Big(2A_{Zh}+\frac{1}{2}C_{F_q}\Big)\Big\}$$

$$C'_9=\frac{V}{gC_0}\left[(C_{m_\alpha}C_{N_\delta}-C_{N_\alpha}C_{m_\delta})(2A_{hh}k^2-C_{F_H})+C_{F_\alpha}(C_{N_\delta}C_{m_H}-C_{m_\delta}C_{N_H})\right]$$

QUASI-STEADY CASE

The coefficients used in the analysis for the quasi-steady case are as follows:

$$\Gamma_0=2\mu K_Y{}^2\Big(2\mu-\frac{1}{2}C_{N_{D\alpha}}\Big)(2A_{hh}k^2-C_{F_H})+A_{\theta h}C_{m_{D\alpha}}C_{N_H}+4\mu K_Y{}^2A_{Zh}C_{N_H}+2A_{\theta h}C_{m_H}\Big(2\mu-\frac{1}{2}C_{N_{D\alpha}}\Big)$$

$$\Gamma'_1=\frac{1}{\Gamma_0}\Big\{\Big[-2\mu K_Y{}^2C_{N_\alpha}-\frac{1}{2}C_{m_q}\Big(2\mu-\frac{1}{2}C_{N_{D\alpha}}\Big)+\frac{1}{2}C_{m_{D\alpha}}\Big(-2\mu-\frac{1}{2}C_{N_q}\Big)\Big](2A_{hh}k^2-C_{F_H})$$
$$+2A_{\theta h}(C_{m_\alpha}C_{N_H}-C_{N_\alpha}C_{m_H})-2A_{Zh}C_{m_H}\Big(-2\mu-\frac{1}{2}C_{N_q}\Big)-C_{m_H}\Big(2\mu-\frac{1}{2}C_{N_{D\alpha}}\Big)\Big(2A_{Zh}+\frac{1}{2}C_{F_q}\Big)$$
$$-C_{N_H}(2\mu K_Y{}^2C_{F_\alpha}+2A_{Zh}C_{m_q})-\frac{1}{2}C_{m_{D\alpha}}C_{N_H}\Big(2A_{Zh}+\frac{1}{2}C_{F_q}\Big)\Big\}$$

$$\Gamma'_2=\frac{1}{\Gamma_0}\Big\{\Big[\frac{1}{2}C_{N_\alpha}C_{m_q}+C_{m_\alpha}\Big(-2\mu-\frac{1}{2}C_{N_q}\Big)\Big](2A_{hh}k^2-C_{F_H})+(C_{N_\alpha}C_{m_H}-C_{m_\alpha}C_{N_H})\Big(2A_{Zh}+\frac{1}{2}C_{F_q}\Big)$$
$$+C_{F_\alpha}C_{m_H}\Big(-2\mu-\frac{1}{2}C_{N_q}\Big)+\frac{1}{2}C_{m_q}C_{F_\alpha}C_{N_H}\Big\}$$

$$\Gamma'_3=\frac{V}{g\Gamma_0}\left[-2\mu K_Y{}^2C_{N_\delta}(2A_{hh}k^2-C_{F_H})+2A_{\theta h}(C_{m_\delta}C_{N_H}-C_{N_\delta}C_{m_H})\right]$$

$$\Gamma'_4=\frac{V}{g\Gamma_0}\Big\{\Big[\frac{1}{2}C_{N_\delta}(C_{m_{D\alpha}}+C_{m_q})-\frac{1}{2}C_{m_\delta}(C_{N_{D\alpha}}+C_{N_q})\Big](2A_{hh}k^2-C_{F_H})$$
$$+2A_{Zh}(C_{m_\delta}C_{N_H}-C_{N_\delta}C_{m_H})+\Big(2A_{Zh}+\frac{1}{2}C_{F_q}\Big)(C_{N_\delta}C_{m_H}-C_{m_\delta}C_{N_H})\Big\}$$

$$\Gamma'_5=\frac{V}{g\Gamma_0}\Big[(C_{N_\delta}C_{m_\alpha}-C_{m_\delta}C_{N_\alpha})(2A_{hh}k^2-C_{F_H})+C_{F_\alpha}(C_{N_\delta}C_{m_H}-C_{m_\delta}C_{N_H})\Big]$$

RIGID CASE

The transfer functions used in the analysis for the rigid case are as follows:

$$K_0=2\mu K_Y^2\left(2\mu-\frac{1}{2}C_{N_{D\alpha}}\right)$$

$$K'_1=\frac{1}{K_0}\left[-\frac{1}{2}C_{m_q}\left(2\mu-\frac{1}{2}C_{N_{D\alpha}}\right)-2\mu K_Y^2 C_{N_\alpha}+\frac{1}{2}C_{m_{D\alpha}}\left(-2\mu-\frac{1}{2}C_{N_q}\right)\right]$$

$$K'_2=\frac{1}{K_0}\left[\frac{1}{2}C_{m_q}C_{N_\alpha}+C_{m_\alpha}\left(-2\mu-\frac{1}{2}C_{N_q}\right)\right]$$

$$K'_7=\frac{V}{gK_0}\left(-C_{N_\alpha}C_{m_\delta}+C_{N_\delta}C_{m_\alpha}\right)$$

$$K'_8=\frac{V}{gK_0}\left[C_{m_\delta}\left(2\mu-\frac{1}{2}C_{N_{D\alpha}}\right)+C_{m_\delta}\left(-2\mu-\frac{1}{2}C_{N_q}\right)+\frac{1}{2}C_{N_\delta}(C_{m_{D\alpha}}+C_{m_q})\right]$$

$$K'_9=\frac{V}{gK_0}\left(-2\mu K_Y^2 C_{N_\delta}\right)$$

APPENDIX C

CONVERSION FACTORS FOR DIMENSIONALIZING THE NONDIMENSIONAL TRANSFER-FUNCTION COEFFICIENTS

The conversion factors for dimensionalizing the nondimensional transfer functions for the semirigid case are as follows:

$$C_1=\left(\frac{V}{\bar{c}}\right)C'_1 \qquad C_5=C'_5$$

$$C_2=\left(\frac{V}{\bar{c}}\right)^2 C'_2 \qquad C_6=\left(\frac{V}{\bar{c}}\right)C'_6$$

$$C_3=\left(\frac{V}{\bar{c}}\right)^3 C'_3 \qquad C_7=\left(\frac{V}{\bar{c}}\right)^2 C'_7$$

$$C_4=\left(\frac{V}{\bar{c}}\right)^4 C'_4 \qquad C_8=\left(\frac{V}{\bar{c}}\right)^3 C'_8$$

$$C_9=\left(\frac{V}{\bar{c}}\right)^4 C'_9$$

The conversion factors for dimensionalizing the nondimensional transfer functions for the quasi-steady case are as follows:

$$\Gamma_1=\left(\frac{V}{\bar{c}}\right)\Gamma'_1 \qquad \Gamma_3=\Gamma'_3$$

$$\Gamma_2=\left(\frac{V}{\bar{c}}\right)^2\Gamma'_2 \qquad \Gamma_4=\left(\frac{V}{\bar{c}}\right)\Gamma'_4$$

$$\Gamma_5=\left(\frac{V}{\bar{c}}\right)^2\Gamma'_5$$

The conversion factors for dimensionalizing the nondimensional transfer functions for the rigid case are as follows:

$$K_1=\left(\frac{V}{\bar{c}}\right)K'_1 \qquad K_7=\left(\frac{V}{\bar{c}}\right)^2 K'_7$$

$$K_2=\left(\frac{V}{\bar{c}}\right)^2 K'_2 \qquad K_8=\left(\frac{V}{\bar{c}}\right)K'_8$$

$$K_3=\left(\frac{V}{\bar{c}}\right)^3 K'_3 \qquad K_9=K'_9$$

REFERENCES

1. Biot, M. A., and Bisplinghoff, R. L.: Dynamic Loads on Airplane Structures During Landing. NACA WR W–92, 1944. (Formerly NACA ARR 4H10.)
2. Donegan, James J., and Huss, Carl R.: Study of Some Effects of Structural Flexibility on the Longitudinal Motions and Loads as Obtained From Flight Measurements of a Swept-Wing Bomber. NACA RM L54L16, 1955.
3. McLaughlin, Milton D.: A Theoretical Investigation of the Short-Period Dynamic Longitudinal Stability of Airplane Configurations Having Elastic Wings of 0° to 60° Sweepback. NACA TN 3251, 1954.
4. Goland, Martin, Luke, Yudell L., and Sacks, Irving: Effects of Airplane Elasticity and Unsteady Flow on Longitudinal Stability. Proj. No. R108E 108 (Contract No. AF 33(038)–2974), Midwest Res. Inst. (Kansas City, Mo.), Oct. 23, 1950.
5. Huss, Carl R., and Donegan, James J.: Method and Tables for Determining the Time Response to a Unit Impulse From Frequency-Response Data and for Determining the Fourier Transform of a Function of Time. NACA TN 3598, 1956.
6. Huss, Carl R., and Donegan, James J.: Tables for the Numerical Determination of the Fourier Transform of a Function of Time and the Inverse Fourier Transform of a Function of Frequency, With Some Applications to Operational Calculus Methods. NACA TN 4073, 1957.

U. S. GOVERNMENT PRINTING OFFICE: 1959